Research Article

Journal of Innate Immunity

J Innate Immun 2018;10:291–305
DOI: 10.1159/000489504

Received: December 5, 2017
Accepted after revision: April 19, 2018
Published online: July 3, 2018

Unique *Francisella* Phosphatidylethanolamine Acts as a Potent Anti-Inflammatory Lipid

Robin Ireland[a] Benjamin Schwarz[a] Glenn Nardone[b] Tara D. Wehrly[a] Corey D. Broeckling[c] Abhilash I. Chiramel[d] Sonja M. Best[d] Catharine M. Bosio[a]

[a]Immunity to Pulmonary Pathogens Section, Laboratory of Bacteriology, Rocky Mountain Laboratories, NIAID, NIH, Hamilton, MT, USA; [b]Research Technologies Branch, NIAID, NIH, Bethesda, MD, USA; [c]Proteomics and Metabolomics Facility, Department of Microbiology, Immunology and Pathology, Colorado State University, Fort Collins, CO, USA; [d]Innate Immunity and Pathogenesis Section, Laboratory of Virology, Rocky Mountain Laboratories, NIAID, NIH, Hamilton, MT, USA

Keywords
Bacteria · Phosphatidylethanolamine · Inflammation · Macrophage · Dendritic cell

Abstract
Virulent *Francisella tularensis* subsp. *tularensis* (Ftt) is a dynamic, intracellular, bacterial pathogen. Its ability to evade and rapidly suppress host inflammatory responses is considered a key element for its profound virulence. We previously established that Ftt lipids play a role in inhibiting inflammation, but we did not determine the lipid species mediating this process. Here, we show that a unique, abundant, phosphatidylethanolamine (PE), present in *Francisella*, contributes to driving the suppression of inflammatory responses in human and mouse cells. Acyl chain lengths of this PE, C24:0 and C10:0, were key to the suppressive capabilities of *Francisella* PE. Addition of synthetic PE 24:0–10:0 resulted in the accumulation of PE in host cells for up to 24 h of incubation, and recapitulated the inhibition of inflammatory responses observed with native Ftt PE. Importantly, this novel PE significantly inhibited inflammatory responses driven by a medically and globally important flavivirus, dengue fever virus. Thus, targeting these lipids and/or the pathways that they manipulate represents a new strategy to combat immunosuppression engendered by Ftt, but they also show promise as a novel therapeutic intervention for significant viral infections.
© 2018 S. Karger AG, Basel

Introduction

Modulation of inflammation is an important feature of both infectious and noninfectious pathological conditions. The mechanisms by which microorganisms influence the inflammatory response is an area of intense study. Defining microbial products and the means by which pathogens exert pressure on the host will aid in the development of novel therapeutics and vaccines.

Although proteins represent a cadre of well-studied virulence factors, other components of pathogens such as lipids and carbohydrates significantly contribute to the disease process. In some cases, these elements trigger a strong inflammatory response, e.g., lipopolysaccharide (LPS) is associated with many gram-negative bacteria. However, lipids have also been found to limit inflammation following infection. For example, lipids derived from

R.I., B.S., and C.M.B. contributed equally to this work.

KARGER

© 2018 S. Karger AG, Basel

E-Mail karger@karger.com
www.karger.com/jin

Dr. Catharine M. Bosio
Immunity to Pulmonary Pathogens Section
Laboratory of Bacteriology, Rocky Mountain Laboratories, NIAID/NIH
903 S. 4th Street, Hamilton, MT 59840 (USA)
E-Mail bosioc@niaid.nih.gov

Table 1. Primers utilized for generation and confirmation of the SchuS4Δ*pcs* mutant

PCS1	GGG**GTCGAC**TCATCGGGCGCTCTTAAGAC
PCS2	GGG**GGATCC**CATTTTAATATTAACTTTTA
PCS3	GCCAAATAGAAGATTTATTAG
PCS4	GCTTAGTGATAATTTGTGTG
PCS5	GATACCGCTCGCCGCAGCCG
PCS6	GGGGGATCCTAATCTGTTTACCTCTTAATC
PCS7	GCGGAGCTCCATCAGACTTAACGATTACCC
PCS8	CCAAGCTCTTGCAAGTCTAG
PCS9	CCCATATAAACATAAGATTC
PCS10	CATTAATGGGATTAAAAGACGC
PCS11	ATCAGCTCACTCAAAGGCGG
PCS12	GG**GACGTC**GATTAAGCATTGGTAACTGT-CAGACC
PCS13	CTAGCTAGCAGGAGACATGAACGATGAACATC
PCS14	GGGACGTCGGATTCACCTTTATGTTGATAAG
PCS15	GTAAGGTTATCAGACTTAAT
PCS16	CGAGGAATCTTATGTTTATA
PCS17	CTAGAAGATAAACAACTATTAC
PCS18	GGGTAAATCTAGATCGTTAG

the parasite *Leishmania donovani* have been documented to drive anti-inflammatory responses in host cells [1].

Francisella tularensis is a gram-negative, facultative, cytosolic, intracellular pathogen, and the causative agent of the lethal disease tularemia. It is highly infectious. In experimental animal models, exposure to as few as 10 organisms results in uniform lethality [2]. In humans, medical intervention was required among volunteers experimentally exposed to aerosols containing 10–15 bacteria [3]. With its high infectivity and ease of aerosolization, *F. tularensis* subsp. *tularensis* (Ftt) was developed as a potential biological weapon, and has since been categorized as a Tier 1 select agent in the USA [4]. Ftt is readily found in the environment as both a free-living and arthropod-transmitted pathogen [5, 6]. Thus, this bacterium also represents a persistent public health threat in both developed and underdeveloped areas of the world [7, 8].

Unlike many other gram-negative bacteria, the primary mechanism of virulence for this organism is its ability to both evade and suppress inflammatory responses, often delaying its identification as the causative agent of disease. Therefore, while Ftt infection can successfully be treated with antibiotics, if exposure to the bacterium was unknown prior to the onset of symptoms, a delayed delivery of therapeutics may not be an effective intervention. Moreover, recrudescence of Ftt infection among individuals completing an antibiotic regime has also been documented [9]. The components and mechanisms responsible for this immunosuppression are not well-defined.

We previously established that nonproteinaceous components, e.g., the lipids and capsule derived from Ftt, play an integral role in dampening the host inflammatory response [10–12]. However, we did not identify the lipid species responsible for inhibiting the inflammatory response. In an earlier work, we confirmed that LPS and, by extension, lipid A derived from Ftt, were neither stimulatory nor anti-inflammatory, suggesting that the immunomodulatory lipid present in Ftt was not a typical TLR antagonist [13]. Thus, we took a systematic approach, utilizing a variety of biochemical techniques to isolate and identify lipids from virulent *F. tularensis* that contribute to the suppression of inflammatory responses in primary mouse and human cells. Importantly, we provide evidence that natural and synthetic versions of these lipids may be effective, novel, anti-inflammatory therapeutics for viral infection.

Materials and Methods

Bacteria

Virulent Ftt strain SchuS4 (SchuS4) was originally provided by Dr. Jeannine Peterson (Centers of Disease Control, Fort Collins, CO, USA). Bacteria were propagated either on modified Mueller Hinton agar or modified Mueller Hinton broth as previously described [13].

Generation of Phosphatidylcholine Synthase Mutant

The phosphatidylcholine synthase (PCS) gene (*FTT_1563*) of Ftt was removed by allelic exchange. Briefly, the 1-kb 5′ region adjacent to *FTT_1563* was amplified with primers PCS1 and 2, and cloned into the previously described pJC84 vector via restriction with *Bam*HI and *Sal*I [14]. Primer sequences used to screen clones are listed in Table 1. Positive clones were confirmed by sequencing with primers PCS3–5. The 750-bp 3′ region adjacent to *FTT_1563* was amplified with primers PCS6 and 7, and cloned via restriction with *Bam*HI and *Sac*I into the 5′ region containing the pJC84 vector. Positive clones were selected by colony PCR with primers PCS5 and 8, and confirmed by sequencing with primers PCS5, 8, 9, and 10. The resultant pJC84Δ1563 vector was transformed into electrocompetent Ftt SchuS4 as previously described, and positive colonies were selected for on kanamycin (Kan)-containing MMH plates. Kan-resistant colonies were screened via colony PCR with primers PCS11 and 12 and PCS13 and 14. Kan-resistant colonies were counterselected in sucrose-containing media, and sucrose-resistant colonies were checked for Kan sensitivity. Kan-sensitive and sucrose-resistant clones were screened for successful deletion via colony PCR with primers PCS15 and 16 and for the correct locus with primers PCS17 and 18.

Crude Lipid Extraction

Lipids were isolated from SchuS4 as previously described [11] with the following modifications. Briefly, after growth on MMH

agar for 48 h, bacteria were collected from the agar plates and mixed with 6 mM Tris-HCL, 10 mM EDTA, and 2% SDS (pH 6.8) to lyse the bacteria, and then heated overnight at 65 °C to sterilize. Lysates were treated with proteinase K overnight and then subjected to 3 rounds of –20 °C ethanol (EtOH) precipitation in the presence of 1 M of sodium acetate. The resultant precipitate was processed using a Folch extraction and the organic phase dried under nitrogen. Dried lipids (crude) were weighed,reconstituted in absolute EtOH (Warner-Graham) to 20 mg/mL, and stored at 4 °C.

Generation of Human Dendritic Cells

Primary human dendritic cells (hDC) were differentiated from apheresed monocytes as previously described [11]. Human monocytes, enriched by apheresis, were obtained from peripheral blood provided by the Department for Transfusion Medicine and the Clinical Center at the National Institutes of Health (NIH; Bethesda, MD, USA) under a protocol approved by the NIH Clinical Center Institutional Review Board. Signed, informed consent was obtained from each donor acknowledging that their donation would be used for research purposes by intramural investigators throughout the NIH.

Mice

C57Bl/6J (B6) female mice (aged 6–8 weeks) were purchased from Jackson Laboratories (Bar Harbor, ME, USA). They were housed in specific pathogen-free conditions in sterile microisolator cages in ABSL-2 facilities at Rocky Mountain Laboratories, and all studies were approved and conducted in accordance with their Animal Care and Use Committee.

Generation of Bone Marrow-Derived Macrophages

Mouse bone marrow-derived macrophages (BMDM) were generated as previously described [15]. Briefly, progenitor cells isolated from the femurs of the indicated strains of mice were cultured in DMEM supplemented with 10% heat-inactivated FCS, 0.2 mM L-glutamine, 1 mM HEPES buffer, and 0.1 mM nonessential amino acids (all from Invitrogen, Carlsbad, CA) (cDMEM), and 10 ng/mL M-CSF (Peprotech) in a T-75-cm^2 flask. On day 2 of culture, nonadherent cells were collected, placed in a fresh T-75-cm^2 flask, and replenished with fresh medium. Adherent cells were collected on day 5, resuspended at 2×10^5 cells/mL and seeded at 0.5 mL/well into a 48-well tissue culture plate with or without glass coverslips. All bone marrow-derived cells were used on day 6 of culture.

Stimulation of hDC and BMDM

Crude lipids, thin-layer chromatography (TLC) bands, and silica fractions isolated from SchuS4 were dried and weighed prior to resuspension in EtOH at a desired concentration before dilution in cRPMI or cDMEM prior to adding to hDC or BMDM, respectively. Synthetic PEPC was dissolved in 5% dextrose in water (D5W) before sonication and dilution into cRPMI or cDMEM. Lipids and vehicle controls were added to hDC or BMDM as indicated, and incubated for 24 h. As indicated, vehicle controls consisted of either EtOH (crude lipids, TLC products, or silica fractions), or D5W (liposomes) diluted the same as the highest concentration of corresponding lipid tested in each experiment. *Escherichia coli* LPS O127:B8 (5 ng/mL) (Sigma) or R848 (5 ng/mL) (Enzo Lifesciences, Farmingdale, NY, USA) was then added to the hDC or BMDM cultures, respectively. Cells were cultured for an additional 20 h before supernatants were collected for the assessment of cytokines. Cell death was assessed by LDH release using a CytoTox 96 nonradioactive cytotoxicity assay according to the manufacturer's instructions (Promega, Madison, WI, USA) and trypan blue staining.

Lipid Analysis Materials

Analytical TLC plates were from Sigma-Aldrich (St. Louis, MO, USA) and preparative TLC plates (1,000 μm, 20 × 20 cm) were from Analtech (Newark, DE, USA). Aminopropyl silica was from Phenomenex (Torrance, CA, USA) and silica gel solid-phase extraction columns from Waters (Milford, MA, USA). Primuline, ninhydrin, copper sulfate, isopropanol, acetone, hexane, ethyl acetate, and triglyceride standards were from Sigma-Aldrich, chloroform (Chl) from Macron (Center Valley, PA, USA), and methanol (MeOH) from Burdick Jackson (Muskegon, MI, USA). Phospholipid standards and synthetic phosphatidylethanolamine (PE) and phosphatidylcholine (PC) were purchased from Avanti Polar Lipids (Alabaster, AL, USA).

Preparative TLC

Crude lipid extract was dissolved in Chl to a concentration of approximately 100 mg/mL. Ten milligrams of sample were applied in a narrow, 8-cm-long zone on the original. An equal volume of pure solvent was applied in the same way adjacent to the sample as a control. The plate was placed in ethyl acetate:MeOH (3:2), and solvent was allowed to move 0.5 cm past the original. The plate was dried, developed with Chl:MeOH:H_2O (7:3:0.25) and dried again. Lipid bands were visualized by spraying the plate with primuline and exposure to fluorescence with long-wavelength UV. Bands were excised with a scalpel and the silica was mixed in 4 mL Chl:MeOH (1:1) for 2 h in sealed glass vials. Negative controls were generated by processing silica sections that were excised from equal areas of silica adjacent to the sample bands. The slurry was filtered on a fritted glass funnel, and the silica was washed with 2 mL of ethyl acetate followed by 2 mL of MeOH. The filtrates were combined, filtered through 0.2-μm regenerated cellulose filters, and the solvent evaporated under an argon stream. The residue was stored under argon at –20 °C.

Fractionation by Solid-Phase Extraction

Fractionation of crude lipid into 3 classes was based on the method of Kaluzny et al. [16]. One milliliter of 25 mg/mL of crude lipid in Chl was gravity-loaded onto a 2-g aminopropyl silica column previously washed with 15 mL of hexane. After complete entry into the bed, hexane was eluted with brief vacuum suction. The column was sequentially developed with 14 mL of Chl:isopropanol (2:1) (fraction I, FI), 2% acetic acid in diethyl ether (fraction II, FII), and MeOH (fraction III, FIII). The 3 fractions were dried under argon and stored at –20 °C. Further fractionation of the phospholipid class (FIII) was based on the Fauland method with modifications. Briefly, approximately 10 mg of FIII was dissolved in 10 mL of Chl:MeOH (2:1) and loaded onto a 1-g silica extraction column previously washed in the same solvent. The column was then washed with 10 mL Chl:MeOH (2:1). Flowthrough and wash were collected and pooled as silica fraction 1 (SF1). The column was then washed with 10 mL Chl:MeOH (1.5:1) and 10 mL of MeOH was applied. This second fraction (SF2) was collected. Fractions were dried under argon, rehydrated in Chl:MeOH (1:1), and analyzed by TLC as described below.

Analytical TLC

Crude lipid fractions I–III (FI–FIII), obtained from solid-phase extraction, and phosphoplipid standards were analyzed on silica gel plates developed in Chl:MeOH:H_2O (7:3:0.25). After drying, TLC plates were sprayed with primuline, and lipids were visualized by fluorescence using long-wavelength UV. Phospholipids were also visualized by molybdenum blue reaction and PE by spraying additional plates with ninhydrin and heating at 115 °C for 10–15 min.

Separation of Phospholipid Molecular Species by HPLC

HPLC was performed using a 1260 Agilent analytical HPLC fitted with a 2.0 × 100 mm C_{18} Luna column (Phenomenex), with isocratic elution in 94% MeOH:acetonitrile (4:1) 6% H_2O run at 0.3 mL/min with elution monitored by UV-Vis at 208 nm. Dried, pooled PE and PC silica fractions obtained from the analytical TLC were dissolved in 0.25 mL Chl:MeOH (1:1). Aliquots of 25–50 µL were diluted with 4 parts MeOH, injected, and the fractions collected. Separation of highly retained PE and PC species was accomplished after 60 and 80 min, respectively. Under these conditions, PE 10:0/–10:0 and PE 14:0/–14:0 was eluted at 7 and 10 min, respectively. PE 16:0/–16:0 was eluted at 22 min and PE 18:1/–18:1 at 25 min. PE 24:0/–10:0 was eluted at approximately 50 min. PE associated with SchuS4 lipids was resolved into 4 major peaks and PC into 6. Each fraction was dried and weighed prior to resuspension in the indicated solvent.

Mass Spectrometry

Band 4 from preparative TLC of Ftt crude lipid was recovered, dried under nitrogen, and resuspended in Chl. Aliquots were directly infused via electrospray ionization into a Xevo G2 TOF, and analyzed under both negative- and positive-ion conditions. Alternate scans were collected with collision energy ramping for tandem mass spectrometry (MS/MS). For positive-ionization mode, the capillary voltage was 2,200 V, the source temperature 150 °C, and the nitrogen desolvation temperature 350 °C with a flow rate of 800 L/h. For negative-ionization mode, the capillary voltage was 2,000 V, the source temperature 150 °C, and the nitrogen desolvation temperature 350 °C with a flow rate of 600 L/h. Data were analyzed using MassLynx (Waters) and masses were searched against Metlin and LipidMaps libraries.

SF1 (PE) samples from solid-phase extraction were dried under nitrogen. Samples were resuspended in Chl:MeOH (1:1) and diluted 1:100 in MeOH:glacial acetic acid (99:1) with 5 mM ammonium acetate. Samples were directly infused at 10 µL/min into a Sciex 400 QTrap with a Turbo IonSpray™ source in positive-ionization mode. Spectra were collected over a mass range of 400–1,000 U. PE and PC species were identified by assuming neutral loss ions for the major peak of 184 and 141 U, corresponding to the PE and PC head group, respectively. Fatty acid tail lengths were analyzed for each species in negative-ionization mode, with fragmentation spectra collected over a mass range of 100–800 U.

Synthetic Lipids

Synthetic 1-tetracosanoyl-2-decanoyl-sn-glycero-3-phosphoethanolamine (PE 24:0/–10:0), 1-palmitoyl-2-oleoyl-*sn*-glycero-3-phosphoethanolamine (PE 16:0/–18:1), 1,2-dilignoceroyl-sn-glycero-3-phosphocholine (PC 24:0/–24:0), and phospholipid standards were obtained from Avanti Polar Lipids.

Phospholipid suspensions for administration were prepared from 10-mg/mL stocks of lipids in Chl. Lipids were aliquoted into glass vials and dried under nitrogen, either as PE 24:0/–10:0 only, or as an 80:20 mixture of PE 24:0/–10:0 and PC 24:0/–24:0. Samples were resuspended in D5W to a final concentration of 1 mg/mL PE 24:0/–0:0. Lipids were dispersed by scraping, followed by heating at 56 °C, and sonicating with a microtip Qsonica 500 W sonicator (30% amp). Lipids were stable at 4 °C for up to 1 month.

Detection of Cytokines

Cytokines were detected using commercially available kits (all from BD Biosciences) and detection was performed following manufacturer's instructions.

Infection of hDC and BMDM with F. tularensis *SchuS4*

hDC and BMDM were infected with *F. tularensis* SchuS4 as previously described [13, 15]. Briefly, hDCs were removed from their original cultures, centrifuged, and adjusted to 1–2 × 10^7/mL in reserved DC medium. Cells treated with medium alone served as negative controls. Bacteria were added and cells were incubated at 37 °C in 7% CO_2 for 2 h, washed once, then incubated with 50 µg/mL gentamicin (Invitrogen) for 45 min to kill extracellular bacteria. Then cells were washed extensively, adjusted to 5 × 10^5 cells/mL in reserved DC medium, and plated 0.5 mL/well in 48-well tissue culture plates.

For infection of BMDM, host cells were plated in 48-well plates. For microscopy studies, BMDM were plated in 48-well plates containing glass coverslips. Bacteria were resuspended at the indicated MOI in 200 µL cDMEM, added to BMDM cultures, and incubated at 37 °C for 90 min. Media were removed, and fresh cDMEM supplemented with gentamicin (50 µg/mL) was added. Cultures were incubated for an additional 45 min at 37 °C to eliminate extracellular bacteria. Cells were then washed 3 times with DPBS, and reserved cDMEM from the original uninfected BMDM cultures was added back to each well.

Immuofluorescence Microscopy

hDC or BMDM macrophages were exposed to synthetic PEPC liposomes or infected with Ftt in a 24-well format as described above. At the indicated time points, hDC were harvested and adhered to glass slides using Cytospin® and fixed with 3% paraformaldehyde for 20 min at 37 °C. Similarly, BMDM on glass coverslips were washed with DPBS and fixed with 3% paraformaldehyde for 20 min at 37 °C. All cells were permeabilized with 0.3% Triton + 10% horse serum in DPBS for 15 min at room temperature. All subsequent staining steps were conducted in this buffer. Endogenous biotin was blocked using an endogenous biotin blocking kit according to the manufacturer's instructions (Thermo Fisher). For the detection of bacteria, slides or coverslips were stained with AlexaFluor 488-conjugated anti-*Francisella* antibody as previously described [17]. For detection of PE lipids, hDC and BMDM were stained with duramycin LC-biotin conjugate at a final concentration of 200 nM for 30 min at room temperature. Duramycin was detected following the addition of AlexaFluor 568-conjugated streptavidin for 30 min at room temperature. All cells were counterstained with DAPI to detect the nuclei. Coverslips were set in 5 µL of Mowiol and allowed to cure overnight.

Cells were imaged with a Zeiss LSM 710 microscope using Zen software for image collection and analysis. All images were taken of multicell fields and representative images were chosen from >10 fields per sample.

Electron Microscopy

For transmission electron microscopy (TEM), 5 μL of a sample was adsorbed onto a freshly glow-discharged, 200-mesh, formvar-coated copper grid. After 2 min, the liquid was wicked off and the grids were stained with 5 μL of NanoVan (Nanoprobes, Inc. Yaphank, NY, USA) for 1 min. Excess stain was wicked away and the grids were examined at 120 kV on the FEI Tecnai Biotwin (FEI, Hillsboro, OR, USA). Negative-stained TEM images were captured using a Hamamatsu Orca camera system (Advanced Microscopy Techniques Corp., Woburn, MA, USA).

Infection of hDC with Dengue Virus

hDC were pretreated with 10 μg/mL crude SchuS4 lipid or 20 μg/mL synthetic PEPC at 37 °C in 5% CO_2 for 24 h in flasks. Cells treated with D5W served as negative controls. Cells were then centrifuged at 800 rpm for 5 min, the supernatant removed and reserved, and the pellets resuspended in 250 μL of cRPMI. Dengue virus (DENV) serotype 2 (New Guinea C) was added (at a MOI = 1) in a volume of 50 μL. Cells were incubated for 1 h at 37 °C and 5% CO_2, followed by addition of 1 mL DPBS and centrifugation at 800 rpm for 5 min. Supernatant was removed and cells were resuspended in reserved medium and plated at 2×10^5 cells per well in 0.5 mL in 48-well plates. Twenty-four hours later, cell culture medium was collected, centrifuged at 800 rpm for 5 min, and assessed for cytokines as described above. Viral titers were determined as previously described for tick-borne encephalitis virus [18]. Briefly, serial 10-fold dilutions of infected hDC supernatants were added to Vero cell monolayers, followed by addition of 1.5% carboxymethyl cellulose (Sigma) in DMEM containing nonessential amino acids (Gibco), 1% L-glutamine, and 1% penicillin/streptomycin. Seven days after infection, cells were fixed with 10% formalin for 1 h and then stained with crystal violet (Sigma). For each dilution, plaques were counted and averaged before calculating plaque-forming units (PFU) per milliliter.

Statistical Analysis

One-way ANOVA, followed by Tukey's multiple comparisons test with significance determined at $p < 0.05$, was utilized to compare ≥3 groups. Analysis for significance between 2 groups was done using an unpaired Student's t test with significance determined at $p < 0.05$.

Results

Separation of Crude Ftt Lipids

To begin identification of the active lipid species in virulent Ftt SchuS4, we first separated crude preparations of SchuS4 lipids by TLC. Following separation, 4 bands were visualized (Fig. 1a). Lipids were extracted from each band and compared for their ability to impair cytokine secretion by DC. Controls included EtOH diluted similarly to crude lipid, and scrapings from the areas of non-lipid-loaded silica plate that matched the same migration distance of each collected lipid band. None of the extracted lipids triggered secretion of IL-12p40 or TNF-α (data not shown). In response to *E. coli* LPS, cytokine secretion by hDC treated with band 1 was not significantly different from vehicle-treated controls (Fig. 1b). Interestingly, in some donors, controls for band 2 impaired DC activity more potently than its corresponding lipids following the addition of LPS (Fig. 1b), suggesting a contribution of solvent or residual stationary phase at that location. In contrast, lipids extracted from bands 3 and 4 both interfered with the secretion of IL-12p40 and TNF-α by hDC in response to LPS (Fig. 1b). However, similar to the controls for band 2, in some donors, control scrapings for band 3 also impaired the ability of hDC to respond to LPS. Therefore, lipids present in band 4 represented components that impaired host cell inflammatory responses, and were targeted for identification and utilization in downstream applications.

To begin identification of the lipids present in band 4, we first analyzed this band by direct-infusion MS. The dominant mass ion in the positive-ionization mode at m/z 720.560 was consistent with the expected protonated form of PE with a completely saturated combined acyl chain length of 34 carbons (PE 34:0) (Fig. 2a). The secondary ion at 579.533 m/z further supported this identification, corresponding to the neutral loss of the PE head group. Secondary ion signals at m/z of 692.53 and 762.61 suggest PE (32:0) and completely saturated PC with 34 acyl carbons (PC 34:0). The annotation of PE (32:0) was further supported by the secondary ion at 551.505 corresponding to the loss of the head group. High fragmentation energy in positive-ionization mode resulted in enrichment of the neutral-loss head-group (M-141) ions for PE (34:0) and PE (32:0) (Fig. 2b). Fragmentation of the corresponding [M-H]-ion in negative mode allowed for the identification of fatty acid tails. Ions corresponding to C10 (171.141) and C24 (367.375) were detected, and collectively accounted for either PE (34:0) or PC (34:0) (Fig. 2c). Major ion signals under these conditions primarily corresponded to fatty acids with various levels of oxidation; however, these species cannot account for the PE (34:0) or PC (34:0) signals. The position of each acyl tail could not be determined from this dataset; however, further analysis of the PE fractions showed the presence of lyso-PE (24:1) and (22:0), suggesting that the PE (24:0/–10:0) isomer was more likely than the PE (10:0/–24:0) isomer (online suppl. Fig. 1 and 2D; for all online suppl. material, see www.karger.com/doi/10.1159/000489504).

Biochemical analysis suggested that the primary lipid species in band 4 was a unique phospholipid containing very long chain fatty acids (VLCFA). We then set out to further isolate the primary active species of phospholipid. We first fractionated crude-lipid preparations into polar

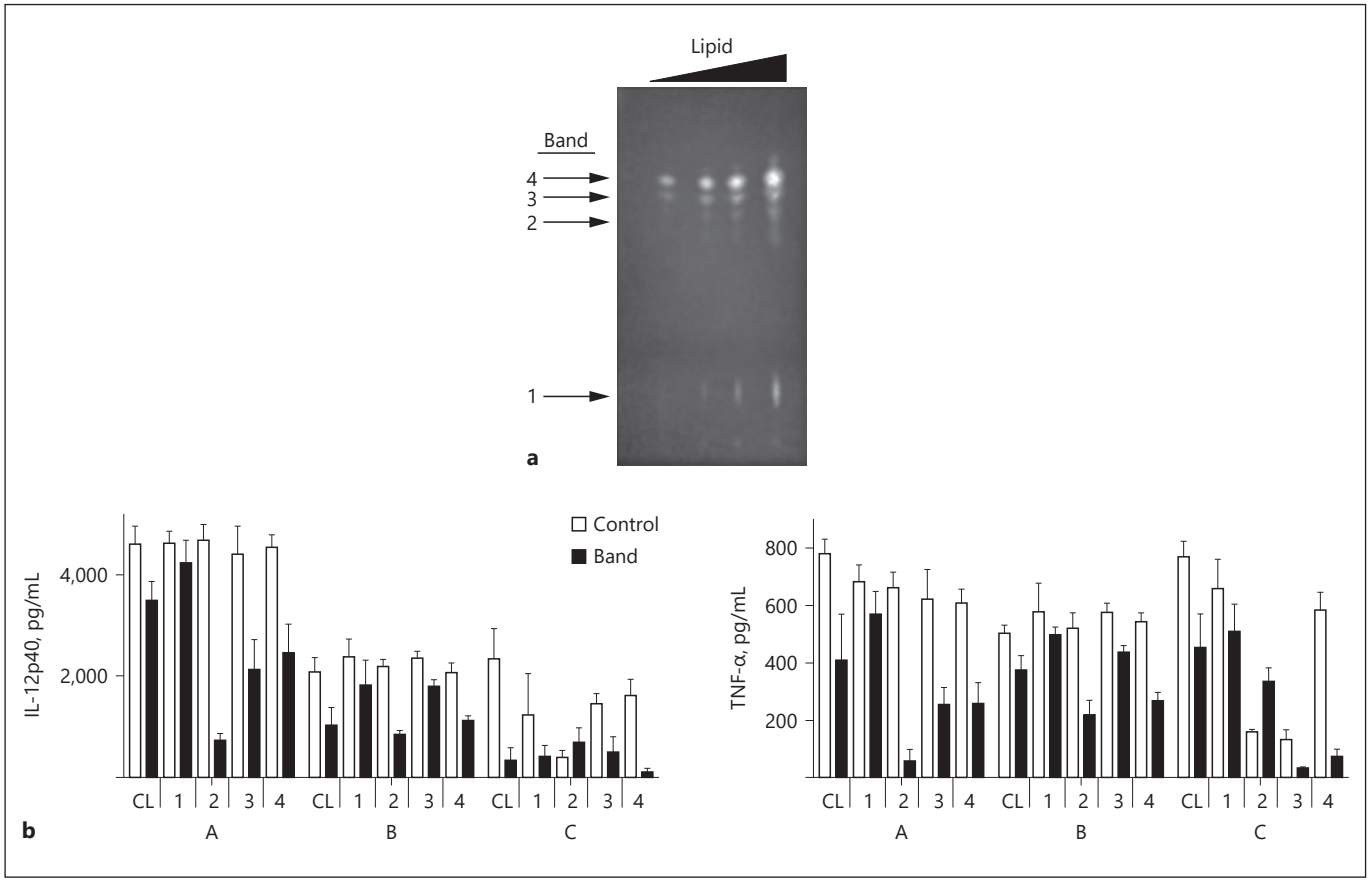

Fig. 1. Comparison of separate lipid species from SchuS4 for anti-inflammatory activity. **a** Separation of crude SchuS4 lipids by TLC. Increasing concentrations of SchuS4 lipids were spotted onto silica plates and separated using ethyl acetate:MeOH (3:2) and Chl:MeOH:H_2O (7:3:0.25) into 4 distinct bands. **b** Each band (1–4) was scraped from the silica plate, processed to remove contaminating silica, and added to human dendritic cells (hDC) at 2 μg/mL (3–4 wells/group), followed by stimulation with *E. coli* LPS (5 ng/mL). Control samples for bands consisted of scrapings from the silica plate adjacent to each sample band. hDC were also treated with 10 μg/mL of crude lipid (CL). Control for crude lipid consisted of EtOH diluted similarly to the lipid. After 24 h, supernatants were assessed for IL-12p40 and TNF-α. Values from the control sample and corresponding band were analyzed using an unpaired, two-tailed, Student's *t* test. A–C indicate individual donors. Error bars represent standard deviation (SD).

molecular classes via solid-phase extraction using aminopropyl silica. This fractionation successfully isolated neutral lipids (FI), free fatty acids (FII), and nonacidic phospholipids (FIII). Acidic phospholipids were likely retained on the column via this method, so we were unable to assess the contribution of these lipid species. We then exposed hDC to each fraction in the presence or absence of LPS. None of the 3 fractions elicited cytokine responses from hDC (data not shown). Depending on the donor, all 3 fractions impaired secretion of TNF-α in hDC exposed to LPS. FII and FIII reproducibly inhibited TNF-α, whereas FI failed to do so in 1 of the donors (Fig. 3a). A similar scenario was observed in samples assessed for IL-12p40. All 3 fractions had some activity, but only FII and FIII were consistently able to inhibit secretion of IL-12p40 in all 3 donors (Fig. 3a). We next separated FI–FIII by TLC and included phospholipid standards for PC and PE. Lipids in FIII migrated similarly to phospholipid standards corresponding to diacyl PC and PE, with no detectable lyso-PE or PC (Fig. 3b). Together, these data suggest that the some of the suppressive lipids present in SchuS4 were phospholipids.

To determine if the primary inhibitory lipids were PE, PC, or both, we further purified FIII by silica solid-phase extraction. The resulting fractions, SF1 (containing PE species) and SF2 (containing PC species), were tested for their ability to inhibit hDC cytokine secretion. Neither fraction elicited detectable cytokine secretion in hDC

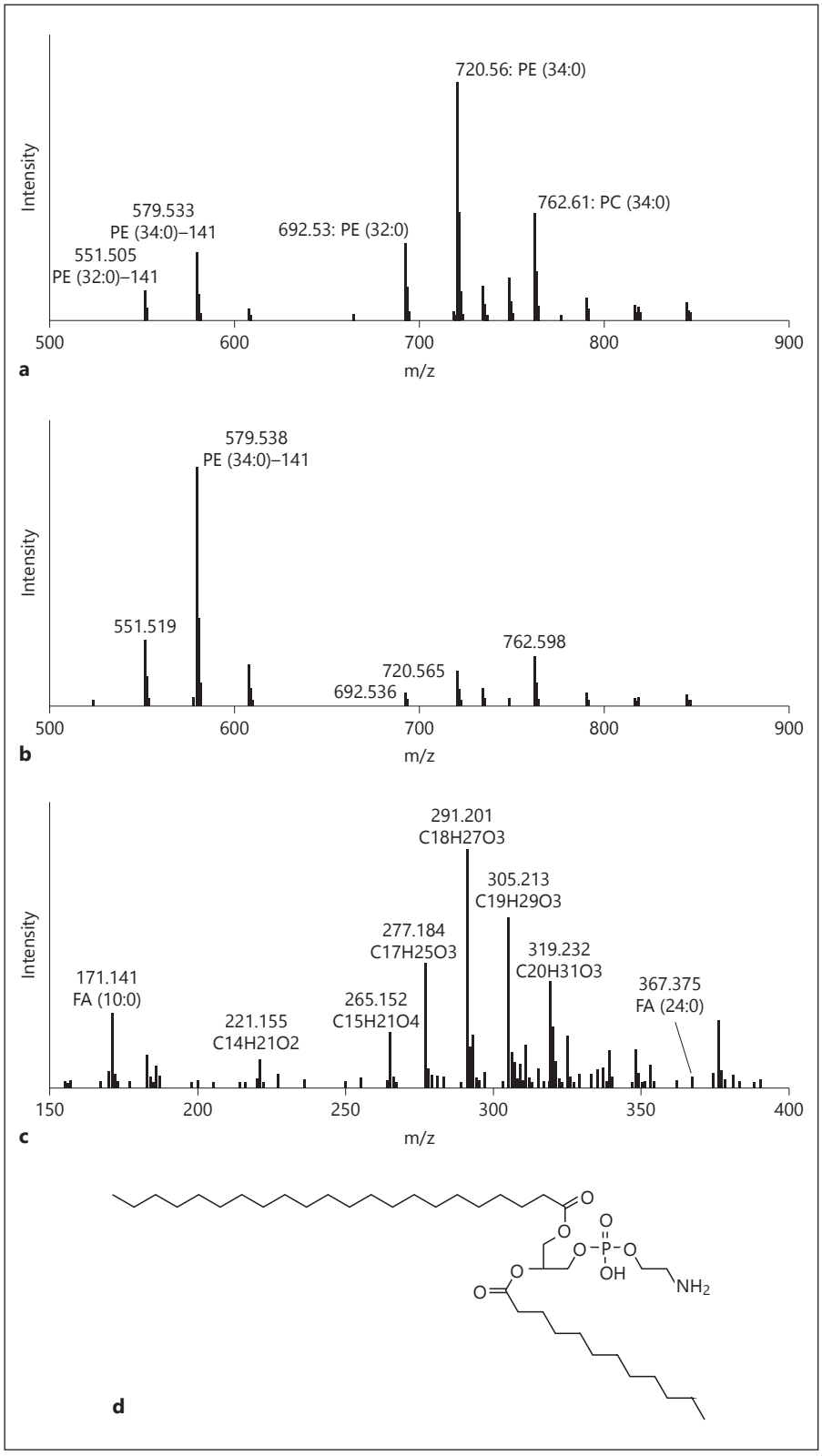

Fig. 2. The major signal from band 4 of crude lipid represents saturated phosphatidylethanolamine (PE) (24:0/–10:0). **a** The dominant mass signal in positive-ionization mode at m/z 720.560 was consistent with the protonated molecular ion for PE with fatty acid chains totaling 34 carbons and zero double-bonds. **b** High-collision energy under positive ionization showed that a major signal at m/z 579.538, consistent with the neutral loss of 141 Da from the 720.560-m/z species which is diagnostic of PE lipids. A concomitant neutral loss from m/z 692 (producing 551) also indicates PE (32:0). A fragment ion at m/z 184 (not shown) also supports the phosphatidylcholine (PC) (34:0) annotation. **c** Negative ionization analysis with high-collision energy conditions revealed several m/z values in the fatty acid (FA) molecular ion mass range. Of these, both saturated C10 (171.141) and C24 (367.375) were observed, which collectively confirms PE (34:0) with a composition of 24:0/–10:0. **d** Suggested structure of PE identified in band 4 of crude SchuS4 lipid.

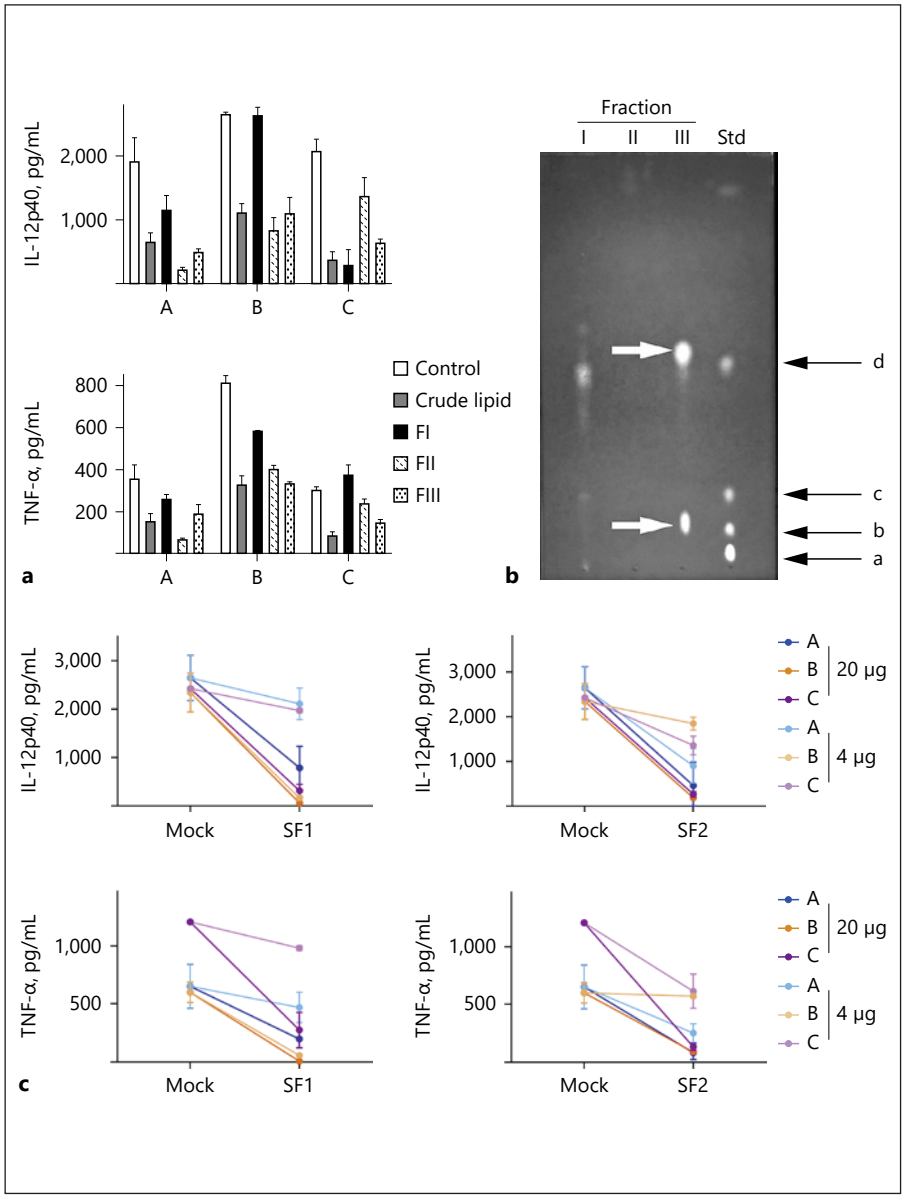

Fig. 3. Phosphatidylethanolamine (PE) and phosphatidylcholine (PC) isolated from SchuS4 impair inflammatory responses in human dendritic cells (hDC). Total lipid from SchuS4 was fractionated into 3 classes (fractions I–III [FI–III]) using aminopropyl silica solid-phase extraction, and these were tested for their ability to inhibit cytokine production in hDC. **a** Each fraction (20 µg/mL) or crude lipid (2 µg/mL) was added to hDC (3–4 wells/group) and incubated overnight. Control samples were treated with EtOH diluted similarly to lipids. hDC were then stimulated with *E. coli* LPS (5 ng/mL), and supernatants were collected the next day to assess TNF-α and IL-12p40. A–C indicate individual donors. Data were analyzed using one-way-ANOVA followed by Tukey's multiple-comparisons analysis. Error bars represent SD. **b** Each fraction was analyzed for lipid content by thin-layer chromatography. The indicated lipid fractions were spotted onto a silica plate and developed with Chl:MeOH:H_2O (7:3:025). Lipid standards (Std), consisting of lyso-PC (a), PC (b), lyso-PE (c), and PE (d) were also added to the plate. Bands were visualized using primuline and UV illumination. The arrow designated as (1) indicates the presence of PE and (2) designates PC in FIII. **c** FIII was further fractionated by silica solid-phase extraction into 2 fractions, enriched for either PE (silica fraction [SF]1) or PC (SF2). SF1, SF2 (at the indicated concentrations), and crude lipid (10 µg/mL) were incubated with hDC overnight, the cells were then stimulated with *E. coli* LPS (5 ng/mL), and supernatants collected the next day to assess TNF-α and IL-12p40. Mock, mock-treated control. A–C indicate individual donors. Error bars represent SD.

cultures (data not shown). Both were able to inhibit IL-12p40 and TNF-α secretion triggered by LPS in hDC when added at 20 µg/mL (Fig. 3c). Depending on the donor, both were also capable of inhibiting cytokine secretion when administered at the lower dose (4 µg/mL). Following the addition of LPS, SF2 showed a dose-dependent inhibition of TNF-α and IL-12p40 (Fig. 3c). Together, these data suggest that both PE and PC species derived from SchuS4 were capable of impairing cytokine production in hDC.

To identify specific species of PE and PC in their respective silica fractions, each fraction was analyzed by direct-infusion MS. This analysis revealed a variety of PE and PC species present in SF1 and SF2. Interestingly, regardless of the phospho head group, nearly all species detected had at least 1 acyl chain containing ≥20 carbons (online suppl. Fig. 1). Similar to the acyl chain lengths observed in PE present in band 4 retrieved from the TLC of crude lipids (Fig. 2), the majority of PE species present in SF1 contained 1 acyl chain of 24:0, 24:1, and 22:0 paired with a second of 10:0 length (online suppl. Fig. 1). This pattern of paired long and short acyl chains was also observed among the PC species present in SF2, where the primary PC species detected consisted of a combination of PC with 24:0/–10:0, 24:0/–8:0, 20:0/–18:1, and 22:0/–18:1 (online suppl. Fig. 1).

J Innate Immun 2018;10:291–305
DOI: 10.1159/000489504

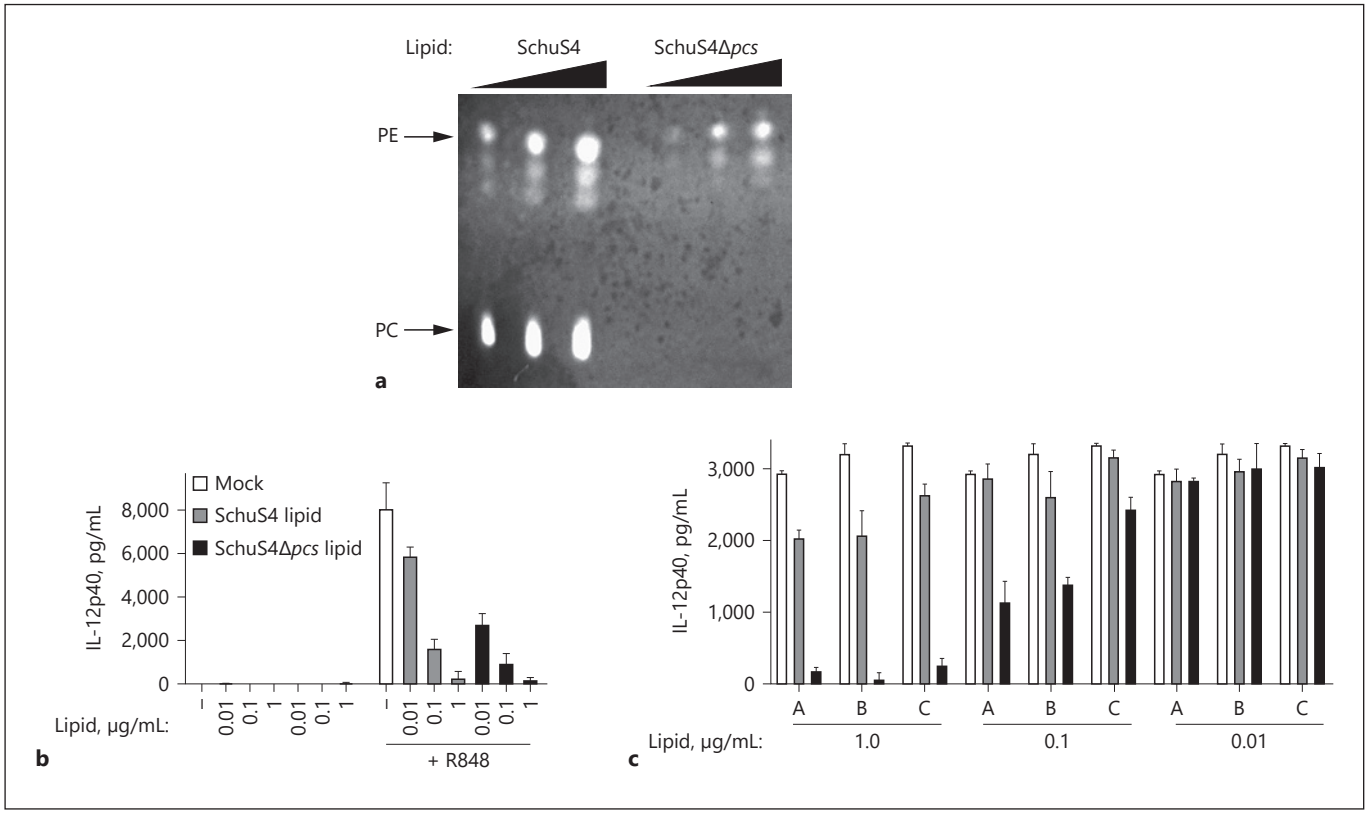

Fig. 4. Phosphatidylcholine (PC) is not required for SchuS4 lipid-mediated inhibition of inflammation in mammalian cells. **a** Confirmation of absence of PC in SchuS4Δ*pcs* mutant. Lipids from wild-type (SchuS4) and SchuS4Δ*pcs* mutant were spotted onto silica plates at increasing concentrations, and developed with Chl:MeOH:H_2O (7:3:0.25). Bands were visualized using primuline and UV illumination. Crude lipids from SchuS4 or SchuS4Δ*pcs* were added at the indicated concentrations to mouse bone marrow-derived macrophages (BMDM) (**b**) or human dendritic cells (hDC) (**c**) (3–4 wells/group), followed by the addition of R848 (5 ng/mL) or LPS (5 ng/mL), respectively. Mock-treated controls (–; Mock) were treated with EtOH diluted similarly to wells containing 1 μg/mL lipid. Supernatants were assessed for IL-12p40 by ELISA. Data were analyzed using one-way-ANOVA followed by Tukey's multiple-comparisons analysis. BMDM data represents 3 experiments of similar design. A–C indicate individual donors. Error bars represent SD.

PC Was Not Required for SchuS4 Lipid-Mediated Inhibition of Host Inflammatory Responses

PE lipids have not been noted to suppress inflammatory responses. In contrast, PC lipids are well-known to negatively modulate inflammation [19]. Thus, it is possible that the Ftt PC (in combination or independently) could inhibit host cell inflammation. To determine if PE or PC species acted in concert or independently to restrain inflammation, we attempted to generate mutants deficient in either PC or PE. The last step in the bacterial synthesis of PE involves the decarboxylation of phosphatidylserine by the enzyme phosphatidylserine decarboxylase. This has been identified as gene *FTT_0384* in *Francisella*. Despite repeated attempts, utilizing a variety of techniques including inducible promoters and repressors, we were unsuccessful in generating a conditional knockout of *FTT_0384*, as it uniformly resulted in a lethal mutation. Given that PE is predicted to comprise >70% of the *Francisella* cell wall, it was not surprising that deletion of a key PE synthesis gene was lethal [20]. Thus, we were not able to evaluate the activity of PC lipids independently of PE. However, it was predicted that *Francisella* was capable of independently producing its own PC by utilizing an encoded PCS gene (*pcs*), *FTT_1563*. We were able to generate a viable mutant with *FTT_1563* deleted. This deletion mutant (SchuS4Δ*pcs*) exhibited no growth defects in broth or cell culture (data not shown). Examination of total lipid extracts by TLC confirmed the absence of PC in the SchuS4Δ*pcs* mutant (Fig. 4a). When compared to immunosuppressive activity of lipids from

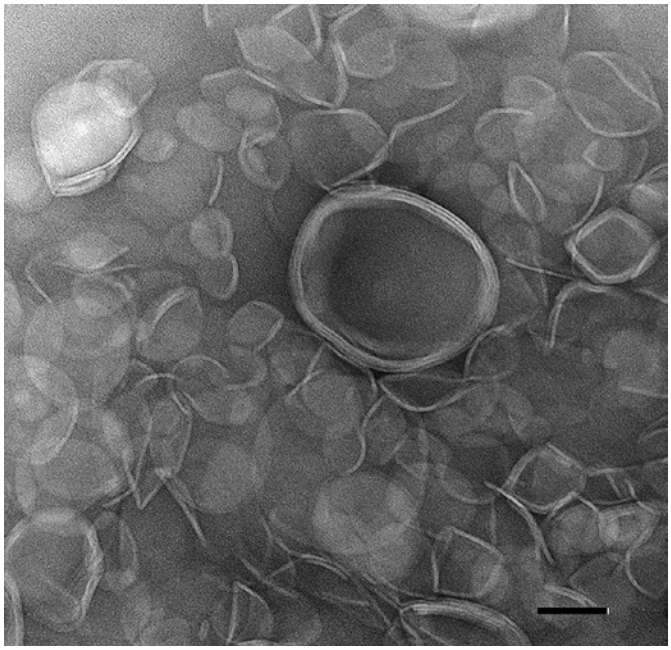

Fig. 5. Synthetic PE liposomes form multilaminar vesicles. Synthetic PEPC liposomes were generated and negatively stained prior to examination by transmission electron microscopy. Scale bar, 100 nm.

wild-type SchuS4, lipids derived from SchuS4Δ*pcs* were significantly better at inhibiting cytokine production from mouse cells (Fig. 4b). This suggested that PC was dispensable for the lipid-mediated inhibition of host inflammatory responses, and that the PE present in SchuS4 did not require the presence of PC to impair inflammatory responses.

Synthetic PE 2410 Inhibits Cytokine Secretion in Primary Human and Mouse Cells

Given the immunomodulatory capabilities of the unique PE we identified in Ftt, we hypothesized that this molecule would be a useful, novel therapeutic for pathological inflammation. There are a number of restrictions and complexities involved in working with virulent Ftt. It was thus desirable to generate a synthetic version of PE 24:0/–10:0 (PE2410) that could be more readily produced under GMP/GLP settings; we therefore had a synthetic version of the unique PE with C24:0 and C10:0 acyl chains (PE2410) generated. As previously described, PE, in general, is highly insoluble, a feature that increases with acyl chain length [21]. A common technique to improve the solubility of PE is to add PC to the PE suspension, resulting in the formation of liposomes. Since we also found long-chain PC species in SchuS4 lipid preparations, we elected to utilize commercially available PC with paired 24 carbon length acyl chains (PC 24:0/–24:0 [PC2424]). After testing various molar ratios, we found the greatest solubility by combining PE2410 with PC2424 at a ratio of 80:20. The resultant liposome formulation was referred to as PEPC2410. We confirmed the generation of liposomes within this formulation utilizing negative-stain TEM. Liposome particles were observed with an approximate particle size distribution of 50–300 nm, and morphologies included single- and multilaminar vesicles (Fig. 5). Liposomes remained stably suspended for many weeks at 4°C.

We then tested the ability of synthetic PEPC2410 to impair inflammatory responses in primary hDC and BMDM. First, we confirmed that any activity observed was not due to the induction of cell death by liposomes or the addition of single phospholipids to cells. We did not observe any increase in cell death, as measured using an LDH assay and trypan blue staining, compared to vehicle-treated controls (data not shown). As controls, we included cells treated with PE containing acyl chains like those that are more typically found in nature (PE 18:1/–16:0 [PE1816]). None of the individual or liposome preparations independently triggered cytokine production from BMDM or hDC (data not shown). PE1816-treated cells also did not show a significant difference in their ability to respond to R848 (a TLR7/8 agonist) or LPS (a TLR4 agonist) compared to vehicle control-treated cells (Fig. 6). Attempts to generate liposomes comprised of PE1816 and PC2424 were not successful as these preparations routinely precipitated out of solution. Therefore, we could not examine the combination of these phospholipids for their ability to impair the production of proinflammatory cytokines. In contrast, both PE2410 alone and in liposome form with PC (PEPC2410) significantly reduced cytokine production in BMDM in response to R848 or LPS, respectively (Fig. 6). Thus, synthetic PE lipids containing very long chain acyl groups modulated inflammatory responses in primary human and mouse cells following exposure to microbial ligands, both as independent ligands and in liposomal form.

Others have described an LPS mimetic that inhibits inflammatory responses in mouse cells via binding and blocking TLR4 on the surface of the host cell [22]. We previously established that TLR4 was not required for the Ftt lipid-mediated inhibition of inflammatory responses [10]. Furthermore, our data also show that Ftt PE and synthetic PEPC2410 impair signaling from TLRs, i.e., TLR7/8, that are not present on the surface of the cell

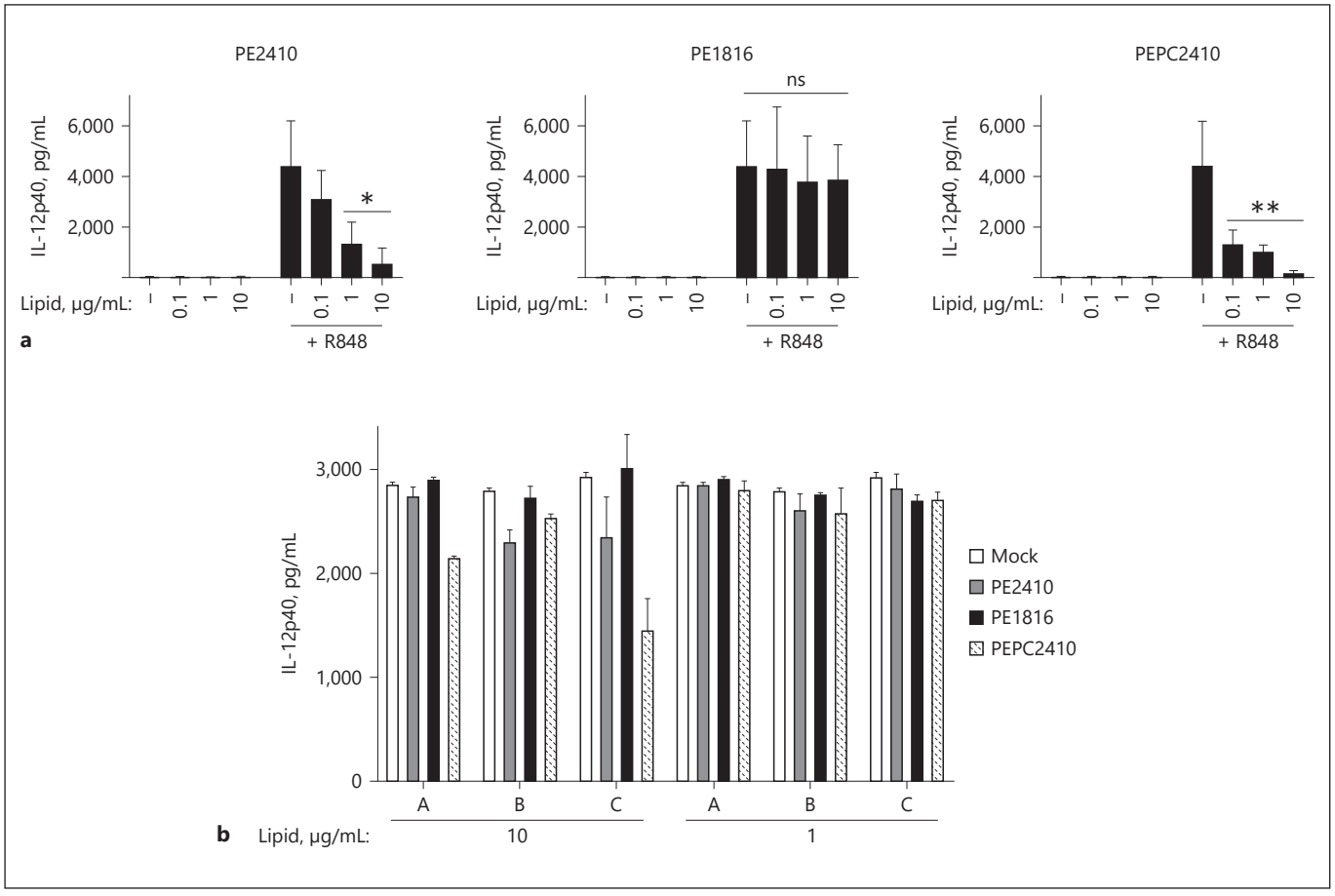

Fig. 6. PE chain length of 24:0/–10:0 is required for inhibition of inflammatory responses in host cells. Individual PE consisting of either 24:0/–10:0 (PE2410) or 18:1/–16:0 (PE1816) or PE liposomes comprising PE2410 and PC 24:0/–24:0 (PEPC2410) were added to mouse bone marrow-derived macrophages (BMDM) (**a**) or human dendritic cells (hDC) (**b**) (3–4 wells/group) at the indicated concentrations and allowed to incubate overnight. hDC or BMDM were then stimulated with *E. coli* LPS (5 ng/mL) or R848 (5 ng/mL), and supernatants were collected the next day to assess IL-12p40. Mock-treated controls (–) were treated with 5% dextrose in water diluted similarly to wells containing 10 μg/mL lipid. BMDM data represent 3 experiments of similar design. A–C indicate individual donors. Data were analyzed using one-way-ANOVA followed by Tukey's multiple comparison analysis. * $p < 0.05$ compared to mock-treated controls and cells treated with 0.1 μg/mL lipid; ** significant compared to mock treated controls; ns, not significant. Error bars represent SD.

(Fig. 6). However, it is possible that Ftt PE plus PEPC2410 may engage other surface structures, allowing adherence to the surface of the cell to impair the interaction and uptake of stimulatory microbial products. Thus, we next determined if the PEPC2410 particles were stuck to the surface of host cells or had been taken up and were present in the intracellular space. Duramycin is a chemical compound that specifically and covalently binds to PE head groups [23]. This allows the detection of PEPC2410 added to hDC and BMDM from mice. One hour after addition, PEPC2410 liposomes were distinguishable in both mouse and human cells as bright puncta against the background of endogenous host cell PE (Fig. 7a). Larger liposomes were visible as rings, suggesting a hollow vesicular structure. PEPC2410 liposomes were visible in cells for up to 24 h after addition to mouse and human cells (Fig. 7a). Together, these data demonstrate that PEPC2410 liposomes were not merely stuck to the surface of the cells, but were readily taken up and persisted in the intracellular compartment of the host cell, regardless of the species of origin of the cell.

We next determined if we could detect and distinguish PE present on the surface of SchuS4 during infection. Following infection of either BMDM or hDC with SchuS4, we detected PE associated with the bacterium, above the background of the host cell PE, that colocalized with

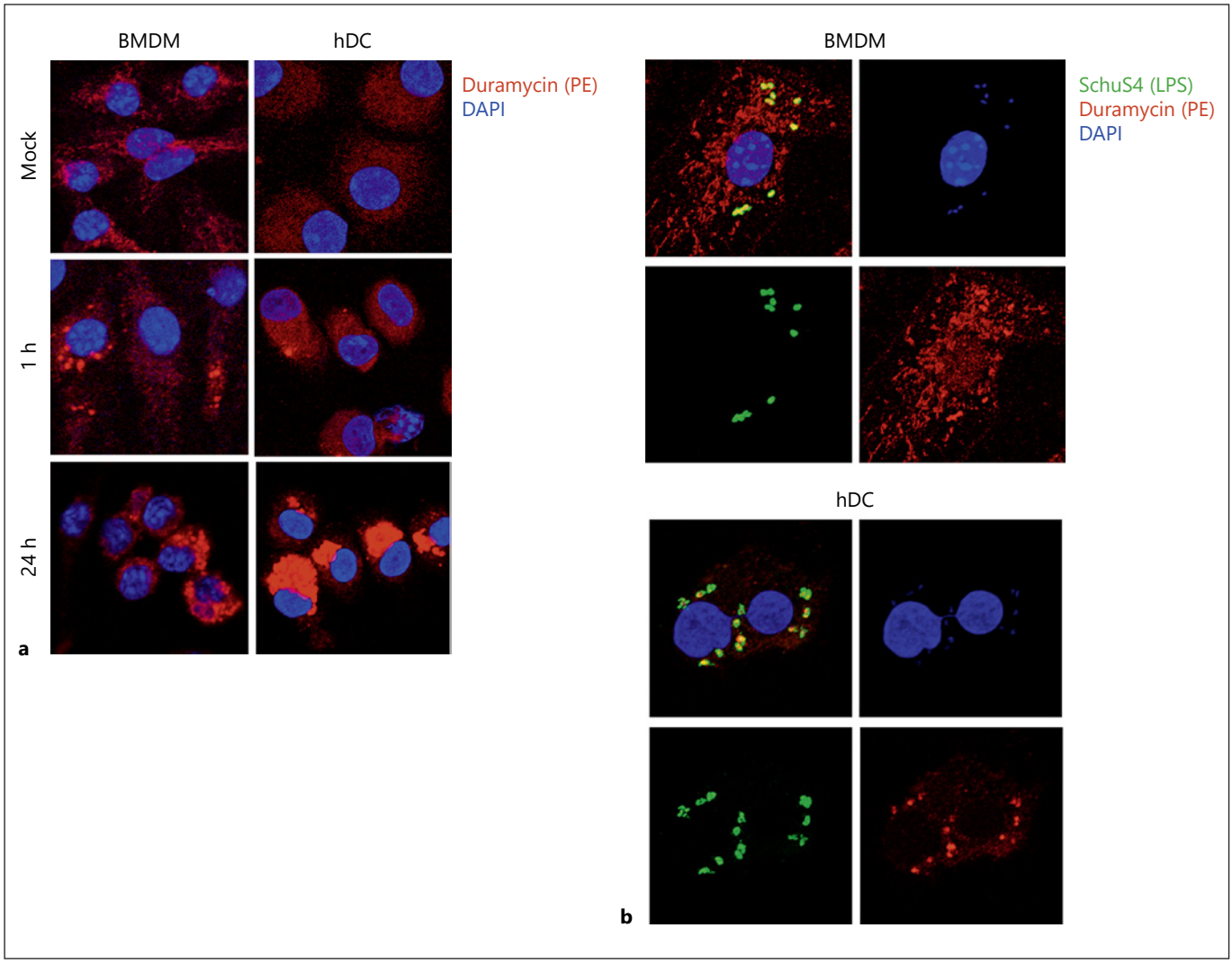

Fig. 7. Detection of PE on synthetic liposomes and viable SchuS4 in the intracellular compartment of host cells. **a** Synthetic PEPC liposomes were generated and added to mouse bone marrow-derived macrophages (BMDM) or human dendritic cells (hDC) (3–4 wells/group) and detected using PE-labeled duramycin 1 and 24 h later. **b** BMDM and hDC (3–4 wells/group) were infected with SchuS4 and PE, and SchuS4 was detected 6 or 8 h after infection, respectively. Data are representative of 3 experiments of similar design.

SchuS4 LPS and DAPI (Fig. 7b). This demonstrated that PE is detectable on intact SchuS4 even after intracellular infection.

PEPC Liposomes Limit Virus-Mediated Inflammatory Responses

Inflammation is required to control and eradicate infiltrating pathogens. However, when inflammation is unconstrained, it can contribute to pathogenesis. There are several examples of aberrant inflammatory responses contributing to morbidity and mortality following viral infection, including infection with DENV, a clinically important arthropod-borne flavivirus [24–26]. Novel therapeutics that target this overzealous inflammatory response, such as those that occur in the context of DENV infection, may reduce morbidity and mortality. Therefore, we tested the ability of crude SchuS4 lipids and synthetic PEPC liposomes to inhibit inflammatory responses following DENV infection of hDC. Both crude SchuS4 lipids and PEPC liposomes inhibited the secretion of IL-6 and TNF-α from DENV-infected hDC when compared to vehicle-treated controls (Fig. 8a). Interestingly, neither

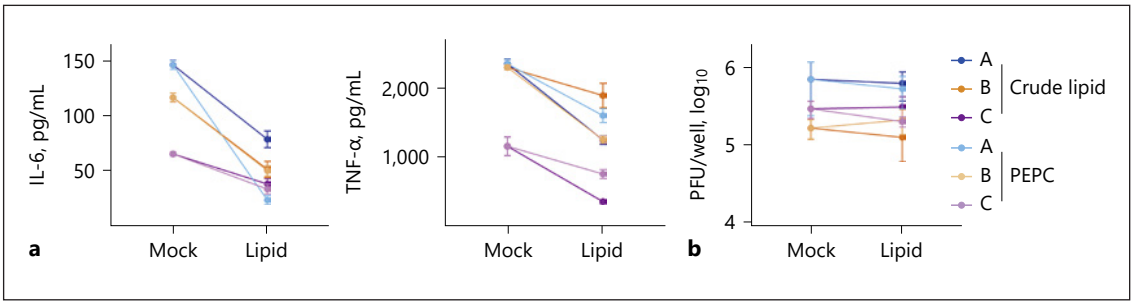

Fig. 8. SchuS4 lipids and synthetic PEPC2410 liposomes inhibit Dengue virus (DENV)-induced inflammatory cytokines. Human dendritic cells (hDC) (3–4 wells/) were treated with crude SchuS4 lipid (10 μg/mL) or synthetic liposomes comprised of PE24:0/–10:0 and PC 24:0/–24:0 (PEPC) (20 μg/mL) overnight. Mock-treated cells (Mock) were treated with 5% dextrose in water. hDC were then infected with (MOI = 1) DENV, and supernatants were collected 24 h later for assessment of IL-6 and TNF-α by ELISA (**a**) and viral load using a plaque assay (**b**). A–C indicate individual donors. Error bars represent SD.

of the lipid preparations significantly impacted viral replication (Fig. 8b). These data suggest that PEPC liposomes may be useful as a therapeutic intervention for virus-mediated inflammation.

Discussion

We identified the immunomodulatory lipids present in virulent *F. tularensis* as PE and PC species consisting of a VLCFA and a shorter fatty acid acyl chain. Both PE and PC enriched from *Francisella* were capable of inhibiting host cell cytokine secretion. However, PC was not required to mediate this effect, as demonstrated by the ability of lipids isolated from a mutant lacking PC (SchuS4Δ*pcs*) to equally impair host cell activity, compared to lipids from wild-type bacteria.

The finding that the most abundant anti-inflammatory lipids derived from Ftt were phospholipids, and included PE, was particularly surprising. To our knowledge, PE derived from bacteria has not been associated with any immunoregulating properties [27]. Rather, these lipids are typically viewed as inert, and not thought to contribute to the recognition of a bacterial pathogen. We indirectly confirmed this phenomenon by demonstrating that PE comprised of the acyl chain combinations more typically found in bacteria, e.g., C 16:0 and C 18:1, neither triggered nor inhibited the production of proinflammatory responses in host cells. The inability of phospholipids comprised of acyl chains consisting of 16 and/or 18 carbons to positively or negatively affect host inflammatory responses also indirectly ruled out Ftt lipid A as a potential immunomodulatory lipid (both when found as part of LPS and in its free state), since its acyl chains consist only of C 16 and C 18 complexes. Together, our data suggest that the presence of a VLCFA chain and/or in combination with a short acyl chain contribute to the immunomodulatory properties of PE and PC found in *Francisella*. Given that it has been approximated that PE comprises around 70% of the bacterial cell membrane, and our data suggest that 75% of the PE found in Ftt consists of combinations of VLCFA and a very short chain fatty acid, these phospholipids are the most abundant lipid in Ftt; they would thus be present at high concentrations following intracellular infection [20].

The presence of VLCFA in *Francisella* has been repeatedly documented in the literature, but the specific lipid species, e.g., phospholipids or lipid A, that carried these acyl chains was not identified [20, 28]. As stated above, the lipid A of *Francisella* sp. is universally comprised of acyl chains consisting of 16–18 carbons. Thus, consistent with our data, *Francisella* lipid A does not contribute to the effects we observed with lipids comprised of VLCFA. One report [29] identified PE lipids isolated from *F. novicida* with lipid chain combinations similar to those observed here. Since *F. novicida* readily triggers an inflammatory response, the presence of PE species in *F. novicida* similar to those found in virulent Ftt was unexpected. However, it is possible that the relative abundance of these specific PE species is different in Ftt and *F. novicida*. In support of this hypothesis, the primary function of PE in bacteria is to provide membrane stability by increasing hydrophobicity, thus allowing organisms to better resist stressful insults. Specifically, bacteria in which PE synthesis has been decreased have greater sensitivity to external stressors such as detergents

and reactive oxygen species [30]. We previously demonstrated that *F. novicida* was significantly more sensitive to reactive oxygen species when it was compared to virulent Ftt [31]; this may be a result of differential ratios of phospholipids in their membranes. We are currently quantifying specific lipid species among strains of *Francisella* to determine if there are correlations with the relative virulence of each bacterium.

The presence of VLCFA in bacteria is highly unusual, with only a handful of prokaryotes documented to possess lipids containing VLFCA [32]. The purpose of VLCFA in bacteria is not clear. To date, the primary function attributed to membrane-associated VLCFA is to increase the rigidity and/or span of the membranes. Our data present a new function of VLCFA in microorganisms, one of immunomodulation. It is not clear how these VLCFA contribute to the impairment of inflammation in host cells. Upon addition of synthetic PE2410 to host cells, we observed an accumulation of PE over time. It is not known if this PE represents the accumulation of PE2410 in the host cells, or if it is newly synthesized host PE. Preliminary experiments in our laboratory suggest that the accumulated PE may be host-derived (data not shown). If this is the case, it suggests that PE2410 was capable of modulating host cell lipid metabolism. Manipulation of lipid metabolism, and more specifically pathogen-directed formation of lipid bodies in host cells, is associated with dampening inflammatory responses. For example, *Trypanasoma cruzi* provokes the formation of lipid bodies upon infection of macrophages [33]. This lipid body formation was associated with the production of PGE_2, a host lipid that interferes with TNF-α and IFN-γ production, 2 cytokines required for the control of *T. cruzi* infection [34]. We have not observed production of PGE_2 following exposure of macrophages or hDC to Ftt lipids, but it is possible that other anti-inflammatory pathways dependent on lipid signaling are activated. We are currently deciphering the metabolic changes triggered by Ftt lipids in host cells to identify the specific mechanism by which these molecules control inflammation.

In addition to representing important virulence factors and (by extension) targets for novel therapeutics following *Francisella* infection, the Ftt lipids identified here may also represent new therapies for disease in which unconstrained inflammation contributes to pathology. One major class of such diseases is virus-mediated infection. Inflammation-driven pathology is associated with many viral infections including, West Nile virus, rabies, and DENV [24, 35, 36]. However, the development of therapeutics for these diseases often focuses on directly targeting the virus rather than the consequence of viral infection, i.e., inflammation. Here, we tested the ability of Ftt lipids to alter the inflammatory responses triggered by infection with an intact virus. Our data suggest that both the natural and synthetic versions of Ftt PE and PC were capable of reducing inflammatory responses in human cells following DENV infection. It is not clear exactly how these lipids shift the inflammatory response during the infection, but, given that we observed that Ftt lipids impair signaling from multiple TLRs present in different cellular compartments, it is not likely that this involves the direct engagement of pattern recognitions receptors. It is known that successful viral infections are intimately tied to host cell lipid metabolism as well as other metabolic pathways [37]. For many viruses, shifting the host cell pathway for cellular-derived energy from oxidative phosphorylation (a relatively anti-inflammatory state) to aerobic glycolysis (which promotes inflammation) is required for optimal viral infection [38]. Preliminary experiments in our laboratory suggest that Ftt lipids can modulate both glycolytic and oxidative phosphorylation pathways in a temporal manner (data not shown). Thus, it is tempting to speculate that Ftt lipids may alter the host lipidome or metabolome to restrict the ensuing inflammatory responses following viral infection.

In summary, we provide evidence that specific PE and PC derived from Ftt can act as immunomodulatory lipids present in these bacteria. In addition to uncovering a novel role for PE possessing VLCFA in the virulence of bacterial infection, we have also established the potential of these lipids to be used in a therapeutic setting for nonbacterial infections. Given the profound ability of Ftt to evade and suppress inflammatory responses in the host, continued identification of its novel virulence factors has the potential for 2 exciting outcomes. First, it will define unexpected targets for combatting this highly pathogenic organism. Second, these molecules could be developed as well-tolerated, potent anti-inflammatory therapeutics for unrelated diseases.

Acknowledgements

This work was supported by the Intramural Research Program of the National Institutes of Health, National Institute of Allergy and Infectious Diseases. Avanti Polar Lipids, Inc. performed mass spectrometry analysis on SF1 and SF2. We also wish to thank Dr. Vinod Nair for assistance in generating the cryoelectron microscopy images.

References

1 Das S, Chatterjee N, Bose D, Banerjee S, Pal P, Jha T, Das Saha K: Lipid isolated from a *Leishmania donovani* strain reduces *Escherichia coli* induced sepsis in mice through inhibition of inflammatory responses. Mediators Inflamm 2014;2014:409694.
2 Molins CR, Delorey MJ, Yockey BM, Young JW, Sheldon SW, Reese SM, Schriefer ME, Petersen JM: Virulence differences among *Francisella tularensis* subsp. *tularensis* clades in mice. PLoS One 2010;5:e10205.
3 McCrumb FR: Aerosol infection of a man with *Pasteurella tularensis*. Bacteriol Rev 1961;25:262–267.
4 Harris S: Japanese biological warfare research on humans: a case study of microbiology and ethics. Ann NY Acad Sci 1992;666:21–52.
5 Petersen JM, Mead PS, Schriefer ME: *Francisella tularensis*: an arthropod-borne pathogen. Vet Res 2009;40:7.
6 Sellek R, Jimenez O, Aizpurua C, Fernandez-Frutos B, De Leon P, Camacho M, et al: Recovery of *Francisella tularensis* from soil samples by filtration and detection by real-time PCR and cELISA. J Environ Monit 2008;10:362–369.
7 Centers for Disease Control and Prevention: Tularemia – United States, 1990–2000. MMWR Morb Mortal Wkly Rep 2002;51:181–184.
8 Hestvik G, Warns-Petit E, Smith LA, Fox NJ, Uhlhorn H, Artois M, Hannant D, Hutchings MR, Mattsson R, Yon L, Gavier-Widen D: The status of tularemia in Europe in a one-health context: a review. Epidemiol Infect 2015;143:2137–2160.
9 Risi GF, Pombo DJ: Relapse of tularemia after aminoglycoside therapy: case report and discussion of therapeutic options. Clin Infect Dis 1995;20:174–175.
10 Crane DD, Ireland R, Alinger JB, Small P, Bosio CM: Lipids derived from virulent *Francisella tularensis* broadly inhibit pulmonary inflammation via toll-like receptor 2 and peroxisome proliferator-activated receptor α. Clin Vaccine Immunol 2013;20:1531–1540.
11 Ireland R, Wang R, Alinger JB, Small P, Bosio CM: *Francisella tularensis* SchuS4 and SchuS4 lipids inhibit IL-12p40 in primary human dendritic cells by inhibition of IRF1 and IRF8. J Immunol 2013;191:1276–1286.
12 Wyatt EV, Diaz K, Griffin AJ, Rasmussen JA, Crane DD, Jones BD, Bosio CM: Metabolic reprogramming of host cells by virulent *Francisella tularensis* for optimal replication and modulation of inflammation. J Immunol 2016;196:4227–4236.
13 Chase JC, Celli J, Bosio CM: Direct and indirect impairment of human dendritic cell function by virulent *Francisella tularensis* Schu S4. Infect Immun 2009;77:180–195.
14 Wehrly TD, Chong A, Virtaneva K, Sturdevant DE, Child R, Edwards JA, et al: Intracellular biology and virulence determinants of *Francisella tularensis* revealed by transcriptional profiling inside macrophages. Cell Microbiol 2009;11:1128–1150.
15 Griffin AJ, Crane DD, Wehrly TD, Scott DP, Bosio CM: Alternative activation of macrophages and induction of arginase are not components of pathogenesis mediated by *Francisella* species. PLoS One 2013;8:e82096.
16 Kaluzny MA, Duncan LA, Merritt MV, Epps DE: Rapid separation of lipid classes in high yield and purity using bonded phase columns. J Lipid Res 1985;26:135–140.
17 Bauler TJ, Chase JC, Wehrly TD, Bosio CM: Virulent *Francisella tularensis* destabilize host mRNA to rapidly suppress inflammation. J Innate Immun 2014;6:793–805.
18 Taylor RT, Lubick KJ, Robertson SJ, Broughton JP, Bloom ME, Bresnahan WA, Best SM: TRIM79α, an interferon-stimulated gene product, restricts tick-borne encephalitis virus replication by degrading the viral RNA polymerase. Cell Host Microbe 2011;10:185–196.
19 Treede I, Braun A, Sparla R, Kuhnel M, Giese T, Turner JR, Anes E, Kulaksiz H, Fullekrug J, Stremmel W, Griffiths G, Ehehalt R: Anti-inflammatory effects of phosphatidylcholine. J Biol Chem 2007;282:27155–27164.
20 Anderson R, Bhatti AR: Fatty acid distribution in the phospholipids of *Francisella tularensis*. Lipids 1986;21:669–671.
21 Yeagle PL, Sen A: Hydration and the lamellar to hexagonal II phase transition of phosphatidylethanolamine. Biochemistry 1986;25:7518–7522.
22 Kim HM, Park BS, Kim JI, Kim SE, Lee J, Oh SC, Enkhbayar P, Matsushima N, Lee H, Yoo OJ, Lee JO: Crystal structure of the TLR4-MD-2 complex with bound endotoxin antagonist Eritoran. Cell 2007;130:906–917.
23 Navarro J, Chabot J, Sherrill K, Aneja R, Zahler SA, Racker E: Interaction of duramycin with artificial and natural membranes. Biochemistry 1985;24:4645–4650.
24 Getts DR, Terry RL, Getts MT, Muller M, Rana S, Deffrasnes C, et al: Targeted blockade in lethal West Nile virus encephalitis indicates a crucial role for very late antigen (VLA)-4-dependent recruitment of nitric oxide-producing macrophages. J Neuroinflamm 2012;9:246.
25 Juffrie M, Meer GM, Hack CE, Haasnoot K, Sutaryo, Veerman AJ, Thijs LG: Inflammatory mediators in dengue virus infection in children: interleukin-6 and its relation to C-reactive protein and secretory phospholipase A2. Am J Trop Med Hyg 2001;65:70–75.
26 Newton AH, Cardani A, Braciale TJ: The host immune response in respiratory virus infection: balancing virus clearance and immunopathology. Semin Immunopathol 2016;38:471–482.
27 Minnikin DE, Abdolrahimzadeh H, Baddiley J: The interrelation of phosphatidylethanolamine and glycosyl diglycerides in bacterial membranes. Biochem J 1971;124:447–448.
28 Jantzen E, Berdal BP, Omland T: Cellular fatty acid composition of *Francisella tularensis*. J Clin Microbiol 1979;10:928–930.
29 Wang XY, Guan ZQ, Li YY, Raetz CRH: Application of electrospray ionization mass spectrometry to characterize glycerophospholipids in *Francisella tularensis* subsp. *novicida*. Int J Mass Spectrom 2010;293:45–50.
30 Rowlett VW, Mallampalli V, Karlstaedt A, Dowhan W, Taegtmeyer H, Margolin W, Vitrac H: Impact of membrane phospholipid alterations in *Escherichia coli* on cellular function and bacterial stress adaptation. J Bacteriol 2017;199:e00849-16.
31 Crane DD, Bauler TJ, Wehrly TD, Bosio CM: Mitochondrial ROS potentiates indirect activation of the AIM2 inflammasome. Front Microbiol 2014;5:438.
32 Rezanka T, Cudlin J, Podojil M: Very-long-chain fatty acids from lower organism. Folia Microbiol 1987;32:149–176.
33 Melo RC: Depletion of immune effector cells induces myocardial damage in acute experimental *Trypanosoma cruzi* infection: ultrastructural study in rats. Tissue Cell 1999;31:281–290.
34 Pinge-Filho P, Tadokoro CE, Abrahamsohn IA: Prostaglandins mediate suppression of lymphocyte proliferation and cytokine synthesis in acute *Trypanosoma cruzi* infection. Cell Immunol 1999;193:90–98.
35 Basu A, Chaturvedi UC: Vascular endothelium: the battlefield of dengue viruses. FEMS Immunol Med Microbiol 2008;53:287–299.
36 Camelo S, Lafage M, Lafon M: Absence of the p55 Kd TNF-α receptor promotes survival in rabies virus acute encephalitis. J Neurovirol 2000;6:507–518.
37 Plaza JJG, Hulak N, Kausova G, Zhumadilov Z, Akilzhanova A: Role of metabolism during viral infections, and crosstalk with the innate immune system. Intractable Rare Dis 2016;5:90–96.
38 Sanchez EL, Lagunoff M: Viral activation of cellular metabolism. Virology 2015;479–480:609–618.